Research Article | Vol. 26, No. 4 | 19 Feb 2018 | OPTICS EXPRESS 3988
Optics EXPRESS

Highly sensitive surface plasmon resonance biosensor based on a low-index polymer optical fiber

SHAOQING CAO,[1,2] YU SHAO,[1,2] YING WANG,[1,*] TIESHENG WU,[1] LONGFEI ZHANG,[1] YIJIAN HUANG,[1] FENG ZHANG,[1] CHANGRUI LIAO,[1] JUN HE,[1] AND YIPING WANG[1]

[1]*Key Laboratory of Optoelectronic Devices and Systems of Ministry of Education and Guangdong Province, College of Optoelectronic Engineering, Shenzhen University, Shenzhen 518060, China*
[2]*These authors contributed equally to this work.*
[*]*yingwang@szu.edu.cn*

Abstract: A highly sensitive refractive index sensor based on surface plasmon resonance in a side-polished low-index polymer optical fiber is proposed for biosensing. Benefitting from the low refractive index of the fiber core, the sensitivity of the device can reach ~44567 nm/RIU theoretically for aqueous solutions, at the expense of a lowered upper detection limit that is down to ~1.340. The sensor is fabricated by coating 55-nm-thick Au-film on the polished surface of a graded-index perfluorinated polymer optical fiber. Results show that the sensor exhibits a sensitivity of ~22779 nm/RIU at 1.335 with a figure of merit of 61.2. When employed for glucose sensing, the sensor presents an averaged sensitivity of 24.50 nm/wt%, or 0.46 nm/mM. This device is expected to have potential applications in cost-effective bio- and chemical-sensing.

© 2018 Optical Society of America under the terms of the OSA Open Access Publishing Agreement

OCIS codes: (060.2370) Fiber optics sensors; (120.0280) Remote sensing and sensors; (280.1415) Biological sensing and sensors.

References and links

1. R. W. Wood, "XLII. On a remarkable case of uneven distribution of light in a diffraction grating spectrum," Philos. Mag. **4**(21), 269–275 (1902).
2. G. Mie, "Beiträge zur Optik trüber Medien, speziell kolloidaler Metallösungen," Ann. Phys. **2330**(3), 377–445 (1908).
3. K. V. Sreekanth, Y. Alapan, M. ElKabbash, E. Ilker, M. Hinczewski, U. A. Gurkan, A. De Luca, and G. Strangi, "Extreme sensitivity biosensing platform based on hyperbolic metamaterials," Nat. Mater. **15**(6), 621–627 (2016).
4. A. Otto, "Excitation of nonradiative surface plasma waves in silver by the method of frustrated total reflection," Z. Phys. **216**(4), 398–410 (1968).
5. E. Kretschmann and H. Raether, "Notizen: Radiative Decay of Non Radiative Surface Plasmons Excited by Light," Z. Natur. A **23**(12), 2315–2316 (1968).
6. B. Liedberg, C. Nylander, and I. Lunström, "Surface plasmon resonance for gas detection and biosensing," Sens. Actuators B Chem. **4**(83), 299–304 (1983).
7. R. C. Jorgenson and S. S. Yee, "A fiber-optic chemical sensor based on surface plasmon resonance," Sens. Actuators B Chem. **12**(3), 213–220 (1993).
8. M. H. Chiu, S. F. Wang, R. S. Chang, and B. C. Sheu, "D-type fiber biosensor based on surface-plasmon resonance technology and heterodyne interferometry," Opt. Lett. **30**(3), 233–235 (2005).
9. W.-H. Tsai, Y.-C. Tsao, H.-Y. Lin, and B.-C. Sheu, "Cross-point analysis for a multimode fiber sensor based on surface plasmon resonance," Opt. Lett. **30**(17), 2209–2211 (2005).
10. K. Gasior, T. Martynkien, M. Napiorkowski, K. Zolnacz, P. Mergo, and W. Urbanczyk, "A surface plasmon resonance sensor based on a single mode D-shape polymer optical fiber," J. Opt. **19**(2), 025001 (2017).
11. L. Coelho, J. M. M. M. de Almeida, J. L. Santos, R. A. S. Ferreira, P. S. André, and D. Viegas, "Sensing Structure Based on Surface Plasmon Resonance in Chemically Etched Single Mode Optical Fibres," Plasmonics **10**(2), 319–327 (2015).
12. L. C. C. Coelho, H. Moayyed, J. L. Santos, and D. Viegas, "Multiplexing of Surface Plasmon Resonance Sensing Devices on Etched Single-Mode Fiber," J. Lightwave Technol. **33**(2), 432–438 (2015).

#318069 https://doi.org/10.1364/OE.26.003988
Journal © 2018 Received 21 Dec 2017; revised 1 Feb 2018; accepted 1 Feb 2018; published 6 Feb 2018

Optics EXPRESS

13. Y. C. Kim, W. Peng, S. Banerji, and K. S. Booksh, "Tapered fiber optic surface plasmon resonance sensor for analyses of vapor and liquid phases," Opt. Lett. **30**(17), 2218–2220 (2005).
14. J. Zhao, S. Cao, C. Liao, Y. Wang, G. Wang, X. Xu, C. Fu, G. Xu, J. Lian, and Y. Wang, "Surface plasmon resonance refractive sensor based on silver-coated side-polished fiber," Sens. Actuators B Chem. **230**, 206–211 (2016).
15. T. Wu, Y. Shao, Y. Wang, S. Cao, W. Cao, F. Zhang, C. Liao, J. He, Y. Huang, M. Hou, and Y. Wang, "Surface plasmon resonance biosensor based on gold-coated side-polished hexagonal structure photonic crystal fiber," Opt. Express **25**(17), 20313–20322 (2017).
16. T. Huang, "Highly Sensitive SPR Sensor Based on D-shaped Photonic Crystal Fiber Coated with Indium Tin Oxide at Near-Infrared Wavelength," Plasmonics **12**(3), 1–6 (2016).
17. Z. Liu, Y. Wei, Y. Zhang, Y. Zhang, E. Zhao, J. Yang, and L. Yuan, "Twin-core fiber SPR sensor," Opt. Lett. **40**(12), 2826–2829 (2015).
18. Y. Wang, J. Dong, Y. Luo, J. Tang, H. Lu, J. Yu, H. Guan, J. Zhang, and Z. Chen, "Indium Tin Oxide Coated Two-Mode Fiber for Enhanced SPR Sensor in Near-Infrared Region," IEEE Sens. J. **9**(6), 1 (2017).
19. P. B. Johnson and R. W. Christy, "Optical Constants of the Noble Metals," Phys. Rev. B **6**(12), 4370–4379 (1972).
20. Y. C. Lin, "Characteristics of optical fiber refractive index sensor based on surface plasmon resonance," Microw. Opt. Technol. Lett. **55**(3), 574–576 (2013).
21. T. Wieduwilt, K. Kirsch, J. Dellith, R. Willsch, and H. Bartelt, "Optical fiber micro-taper with circular symmetric gold coating for sensor applications based on surface plasmon resonance," Plasmonics **8**(2), 545–554 (2013).
22. M. Hautakorpi, M. Mattinen, and H. Ludvigsen, "Surface-plasmon-resonance sensor based on three-hole microstructured optical fiber," Opt. Express **16**(12), 8427–8432 (2008).
23. M. D. Baiad and R. Kashyap, "Concatenation of surface plasmon resonance sensors in a single optical fiber using tilted fiber Bragg gratings," Opt. Lett. **40**(1), 115–118 (2015).
24. https://refractiveindex.info/?shelf=main&book=H2O&page=Hale.

1. Introduction

Plasmonic biosensors have been widely investigated to monitor the concentration of biomarkers and biomolecular interactions in real-time. Typically, the principle of plasmonic biosensing is the excitation and modification of collective charge oscillations in forms of surface plasmon polaritons (SPPs), localized surface plasmons (LSPs) and bulk plasmon polaritons (BPPs) [1–3], since the light field confined in these oscillations is very sensitive to the refractive index (RI) change of surrounding medium. Among these types of oscillations, SPPs are originally proposed for chemical- and bio-sensing with the well-known Kretschmann prism configuration, in which surface plasmon resonance (SPR) can be excited in the vicinity of the metal/analyte interface by the evanescent field of incident light [4–6].

As an alternative to the Kretschmann prism configuration, optical fibers have been considered to be an excellent platform for developing miniaturized and low cost SPR sensors. The fiber core acts as a prism and SPR can be excited by the evanescent field of the confined light once a noble metal layer is introduced in surrounding of the core region. Since the first demonstration of fiber optic SPR sensors [7], numerous designs have been proposed for SPR sensing with modified sensitivities and/or detection limits, mainly employing single mode fibers (SMFs) and multimode fibers (MMFs) accompanied with side-polishing [8–10], chemical-etching [11, 12] and tapering-down treatments [13]. Recently, the diversity of optical fibers, such as D-type fibers [14], photonic crystal fibers [15, 16], twin-core fibers [17], and two mode fiber [18], also enriches the forms of SPR sensors. And a high sensitivity of 6463 nm/RIU (refractive index unit) has been reported for aqueous solution test with an end-face grinded twin-core fiber SPR sensor [17]. And as a novel kind of fiber, two mode fiber is firstly demonstrated to show a sensitivity higher than 10000 nm/RIU, when it is side-polished and coated with a layer of ITO film [18]. However, it is very difficult to further increase the sensitivities of these devices since all of them are realized in silica-based optical fibers, where the phase matching condition between the fiber core mode and surface plasmon (SP) mode limits the RI sensitivity for aqueous solutions. Generally, the sensitivity of fiber SPR sensors increases acceleratory with surrounding RI increasing and approaches infinity when surrounding RI equal to that of the fiber core. For a fixed RI that to be measured, the smaller the difference between this RI and that of the fiber core used, the higher the

Optics EXPRESS

sensitivity is. And the resonant wavelength for the case of higher sensitivity is always longer than that for the case of lower sensitivity. To obtain huge enhancement of RI sensitivity, a feasible and simple scheme is tuning SPR to longer wavelengths. And for biosensing applications, the sensitivity may be greatly enhanced by use of low-index optical fibers with core-RI slightly higher than that of water.

Here we demonstrate a highly sensitive SPR biosensor based on a low-index polymer optical fiber (POF). The sensor was fabricated by side-polishing the POF with a length of ~5 mm to expose the fiber core and coating a 55-nm-thick Au film onto the polished surface. The sensor was tested in the RI range between 1.300 and 1.335 and exhibited a sensitivity of ~22779 nm/RIU at RI value of 1.335. For glucose sensing, the device presented an averaged sensitivity of 24.50 nm/wt%, which reveals that the sensor is meaningful to highly sensitive chemical- and bio-sensing.

2. Principle and fabrication

The principle of the sensitivity enhancement can be simply illustrated with the phase matching conditions for a traditional Kretschmann prism configuration, as depicted in Fig. 1. The SP mode dispersion curves at metal-dielectric interface and metal-prism interface are plotted according to the Drude model [19] for Au-films and labeled as curve *i* and *ii* in Fig. 1, respectively. ω_p is the plasma frequency, and the dispersion curves of SP modes are approaching but not exceeding $\omega_p/\sqrt{2}$ with k (wavenumber) increasing. With neglecting material and waveguide dispersions, the dispersion curves of core mode in silica fiber, CYTOP POF and incident light in air are roughly plotted as line *1*, line *2* and line *3*, respectively. The phase matching condition of SPR is determined by the intersection between the core mode and SP mode dispersion curves. Compared to the intersection *a* between line *1* and curve *i*, intersection *b* between line *2* and curve *i* locates at lower frequencies (or longer wavelengths) and exhibits much bigger slope, which implies that the RI sensitivity of fiber SPR sensor will be dramatically enhanced with employing low-index optical fibers.

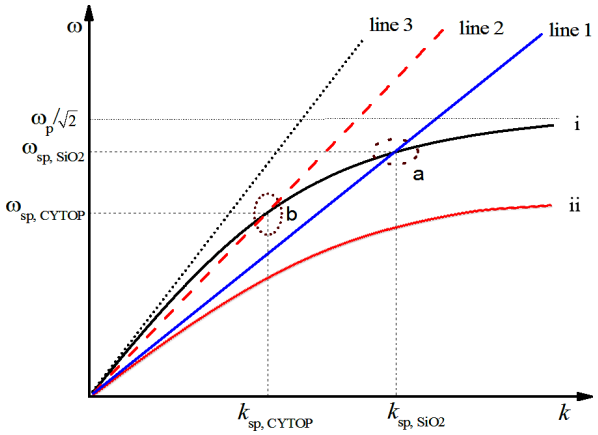

Fig. 1. Dispersion curves for a traditional Kretschmann prism configuration.

In our experiment, a low-index POF (GigaPOF-62SR, Chromis Fiberoptics Inc.) was used to fabricate SPR sensors. The fiber is composed with a graded-index core, cladding and additional reinforcement layer (overcladding), of which the diameters are 62.5, 102.5 and 490 μm, respectively. The cladding and core materials are perfluorinated and doped-perfluorinated optical polymer (CYTOP). It should be noted that single mode CYTOP fibers should better be used, however, it is not commercially available yet. The RI of the core decreases from 1.357 at the fiber center to 1.342 at the core/cladding interface gradually and

Optics EXPRESS

remains unchanged in the cladding, nominated at 589 nm. And the numerical aperture of the fiber is 0.185 ± 0.015.

A wheeled polishing machine was used to polish the POF to a D-shaped geometry [14]. The transmission spectrum can be monitored in real-time by connecting the POF with a broadband light source (BBS, 1250-1650 nm, Fiberlake Inc.) and an optical spectrum analyzer (OSA, YOKOGAWA AQ6370C) during the polishing process. The POF was fast polished by a 3000-grit abrasive paper to remove the protection layer (overcladding) firstly, and then a 7000-grit abrasive paper was used to polish the POF successively until the evanescent field of the guided mode was slightly exposed, which can be determined by observing the appearance of tiny losses in the transmission spectrum. Finally, a 12000-grit abrasive paper was used to modify the polished flat surface carefully for 15 min to suppress the grinded roughness and ensure the uniformity of the evanescent field. The total time consumed for polishing one fiber sample is ~30 min. The insertion loss brought by the polishing process was less than 1 dB, which is required to ensure sufficient high quality spectrum can be obtained, and the thickness of the residual fiber of polished area was ~240 μm with a total length of ~5 mm. The polished POF was coated with Au-film by magnetron sputtering method. The vacuum chamber pressure was evacuated to 5×10^{-4} Pa and then argon filled continuously with a quasi-static pressure of 2 Pa during the Au deposition, and the DC current intensity was set to 36 mA. The deposition rate was 0.07 nm/s. The thickness of gold film deposited on the polished surface of POF was measured to be ~55 nm by step profiler. The top-right inset of Fig. 2 shows the SEM image of the fabricated sensor in cross-section view.

3. Results and discussion

Figure 2 shows the experimental setup for RI measurement with the proposed fiber SPR sensor. Broadband light from a halogen light source was launched into the sensor at one end of the sensor, and the transmitted light from the other end was collected by spectrometer with operating wavelengths from 300 to 1100 nm (QE-6500, Ocean spectra) or from 900 to 1700 nm (NIRQuest512, Ocean spectra) according to the resonant wavelength of the sensor. The transmission spectrum obtained by the spectrometer can be recorded by a personal computer (PC) in real-time and post processed with smoothing algorithms. Two fiber holders were used to keep the sensing area straightly during RI measurements. The transmission spectrum of the device in air was used as a reference spectrum, divided by which normalized transmission spectra can be obtained with the transmission spectra of the device in other analytes. For testing reliability, the sensor was cleaned by anhydrous ethanol carefully until the spectrum recovered to the reference after each test.

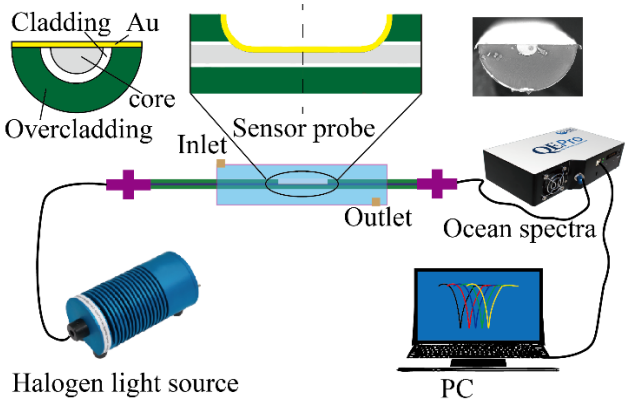

Fig. 2. Schematic diagram of the experimental setup for RI measurements. Insets: cross-section geometry (top-left) and SEM image (top-right) of the sensor.

Optics EXPRESS

The transmission spectra of the proposed sensor in analytes (standard RI liquids, Cargille Lab Inc.) with RI from 1.3000 to 1.3350 are plotted in Fig. 3(a). The resonant wavelength appears at 761 nm with an extinction ratio of 40% for surrounding RI of 1.3000. Note that the theoretical maximum of extinction ratio is 50% for non-polarization maintaining fiber based SPR sensors. With surrounding RI increasing, the SPR resonant dip shifts to longer wavelengths and the extinction ratio decreases gradually. The sensitivity is calculated to be ~5014 nm/RIU at 1.3000-RI, and enhances apparently with surrounding RI increasing and that at 1.3350 reaches to ~22779 nm/RIU, which is one order of magnitude higher than that of conventional SPR sensors based on silica fibers [20, 21]. The relationship between the resonant wavelengths and surrounding RIs are plotted in Fig. 3(b) with black solid squares and the sensitivities are labeled nearby with black numbers. The nonlinearity of sensitivity enhancement is mainly determined by the dispersion characteristics of SP mode at the metal/analyte interface, which is also demonstrated with silica fiber based SPR sensors [14, 15]. It should be noted that the full-width at half-maximum (FWHM) of the SPR resonant dip broadens with the resonant dip shifts to longer wavelengths, which will degrade the figure of merit (FOM) of the device. The FOM can be calculated with the RI sensitivity divided by the FWHM of the resonant dip, which reads 30.2 at 1.3000-RI and approaches to a maximum of 61.8 at 1.3300-RI and then drops due to the resonant dip broadening. Of course, there are still rooms to enhance the FOM, such as using a single mode POF with similar materials to decrease the FWHM of SPR resonant dips.

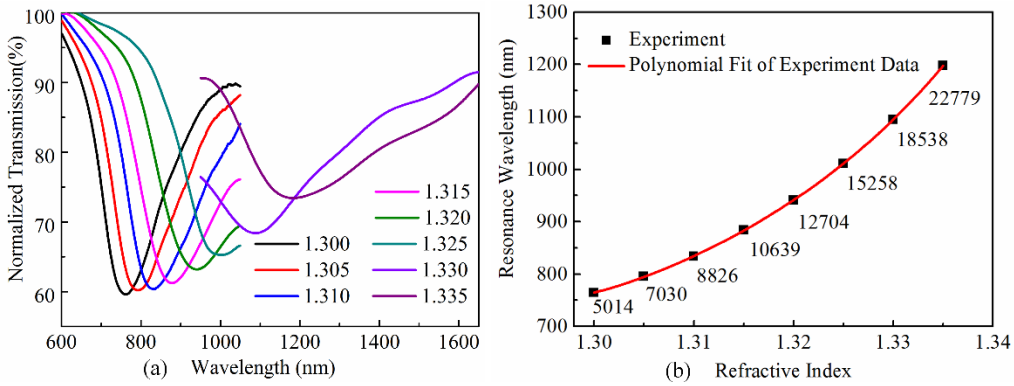

Fig. 3. (a) Experimentally obtained transmission spectra, (b) SPR resonant wavelengths in experiment.

We simulated and analyzed the mode coupling properties and RI response of the proposed sensor by the finite element method [10, 15, 22]. The model was established according to the sensor geometry shown in the top-left inset of Fig. 1. The graded index fiber core with a diameter of 62.5 um was half polished in the model, and the thickness of Au-film deposited on the polished surface was 55 nm according to the experimental data. Meanwhile, the material dispersion of the fiber core (doped CYTOP) was taking into account in the simulation, according to the Cauchy formula:

$$n_{core}=a_1+a_2\cdot\lambda^{-2}+a_3\cdot\lambda^{-4}, \quad (1)$$

where $a_1=1.3504$, $a_2=0.00239$, $a_3=-5.9190\times10^{-5}$, λ is light wavelength (in microns) in vacuum.

The RI of the fiber cladding (pure CYTOP) was assumed constant to be 1.342, and the dielectric constant of the gold film was given by the Drude model [19]. The surrounding RI (n_a) was from 1.3000 to 1.3350 with a step of 0.0050. Since SPPs at the metal/analyte interface can only be excited by the TM-polarized light [23], we just need to track the losses of TM-polarization-like core modes that can cause SPR absorption to determine the resonant

Optics EXPRESS

wavelengths, and only the fundamental core mode of the model was considered for simplicity. According to the computed complex effective RI (n_{eff}) of the TM-polarized fundamental core mode, the confinement losses can be estimated by the following equation [15]:

$$\alpha_{loss} = 8.686 \cdot k_0 \cdot \mathrm{Im}[n_{eff}] (\mathrm{dB/m}), \quad (2)$$

where k_0 is the wavenumber in vacuum with λ being in meters.

The computed loss spectra of the proposed sensor in different surrounding RIs are plotted in Fig. 4(a). SPR resonant wavelengths (λ_{res}) can be treated as the wavelengths with maximum losses in the loss spectra. One can see clearly that λ_{res} moves to longer wavelengths with n_a increasing, and the peak loss decreases and FWHM of the resonance broadens gradually, which agree well with the experimental observation. The relationship between the computed λ_{res} and n_a are also plotted in Fig. 4(b) with red solid circles for comparison with that of experimentally obtained. There is minor discrepancy of the resonant wavelength at 1.300-RI, which is possibly caused by the index difference between the actual value and that obtained from formula (1) for the core material. The computed sensitivities are labeled nearby with red numbers for different RI values, which increases rapidly from 4005 nm/RIU at 1.300-RI to 44567 nm/RIU at 1.335-RI. For surrounding RIs lower than 1.325, the computed RI sensitivities are in good agreement with the experimental results. However, obvious difference can be found between the simulated and experimental ones for surrounding RIs higher than 1.325. This is mainly caused by the dispersion errors between the nominated RIs and the actual values of surrounding analytes and the fiber material at longer wavelengths, since the RIs of the standard RI liquids and the fiber material used in the experiment are nominated at 589 nm. This effect could be further confirmed by subsequent experiments for RI measurement of aqueous solutions.

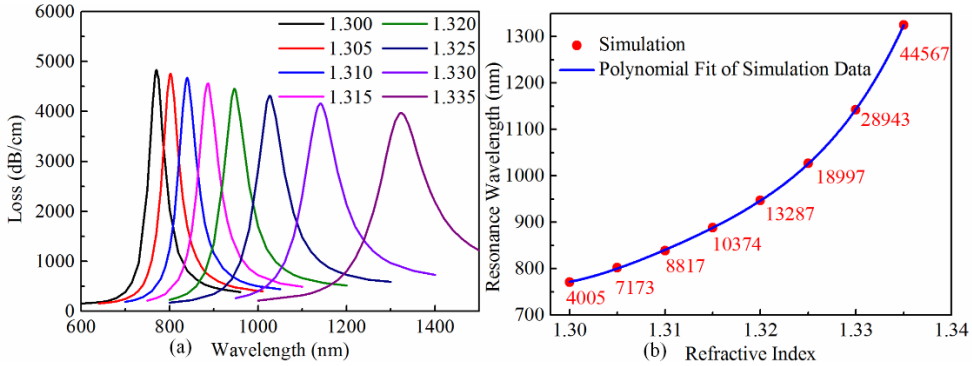

Fig. 4. (a) Simulated loss spectra of the proposed sensor with surrounding RI changing from 1.3000 to 1.3350. (b) SPR resonant wavelengths in simulation.

As the sensor exhibited very high sensitivities for RI ranges of aqueous solutions, it may find important applications in highly sensitive bio-sensing. Here, the device was demonstrated to test the concentrations of glucose solutions in mass fraction, ranging from 0%wt to 5%wt with a step of 0.5%wt. The SPR resonant wavelength appears at 1055 nm in pure deionized water (or 0%wt solution), and shifts to 1184 nm in 5%wt glucose solution. The observed resonant wavelength is shorter than that indicated at 1.333 according to the polynomial fit of the computed results shown in Fig. 4(b), because the actual RI of water is only ~1.324 at 1055 nm [24]. Figure 5 shows the transmission spectra and resonant wavelengths during the concentration test of glucose solutions. The relationship between the resonant wavelength and glucose concentrations is fitted linearly with a goodness coefficient

Optics EXPRESS

R = 0.994 and exhibits an averaged sensitivity of 24.50 nm/wt%, or 0.46 nm/mM, which corresponds to a RI sensitivity of 17560 nm/RIU according to the simulation results.

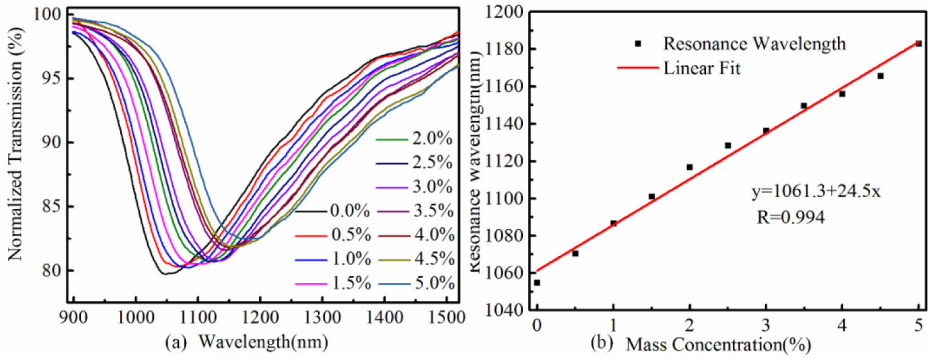

Fig. 5. (a) Normalized transmission spectra and (b) resonant wavelengths of the SPR sensor for different mass concentrations of glucose solutions.

4. Conclusion

In summary, we have proposed a low-index polymer optical fiber based SPR sensor for highly sensitive bio-sensing. The sensor employs a traditional Kretschmann prism configuration, realized by coating an Au-film onto the flat surface of a side-polished POF. Both theoretical and experimental analysis of the RI sensitivity of the proposed sensor were conducted, and results showed that the sensitivity can reach 44567 nm/RIU theoretically and 22779 nm/RIU experimentally for RI equals to 1.3350, respectively. For glucose sensing, the sensor also presented very high sensitivity of 24.50 nm/wt%, or 0.46 nm/mM. Meanwhile, the device is robust due to the good elasticity of the POF used. The proposed sensor is expected to find potential applications in highly-sensitive, cost-effective bio- and chemical-sensing.

Funding

National Natural Science Foundation of China (NSFC) (grant nos. 61675137, 61425007 and 61635007); Guangdong Natural Science Foundation (grants no. 2015B010105007, 2014A030308007 and 2015A030310243); Education Department of Guangdong Province (grant no. 2015KTSCX119); Science and Technology Innovation Commission of Shenzhen (grants nos. JCYJ20160307143501276 and JCYJ20160427104925452); Development and Reform Commission of Shenzhen Municipality foundation; Open Fund of the Guangdong Provincial Key Laboratory of Optical Fiber Sensing and Communications (Jinan University).

58.60.63.193 {ts '2018-02-06 21:27:54'}